Application of the Photoacoustic technique in the optical and thermal characterization of a ternary compound embedded in a zeolite host

A. Hernández-Guevara, A. Cruz-Orea and F. Sánchez-Sinencio
Departamento de Física, CINVESTAV-IPN. A. P. 14-740 México D.F. 07000, México. Tel. (+52) 5 747 38 00 exts. 6171,6191. Fax: (+52) 5 747 70 97. E-mail: aleher@fis.cinvestav.mx and orea@fis.cinvestav.mx

O. Vigil[a]
Escuela Superior de Física y Matemáticas, IPN, Unidad Profesional Adolfo Lopez Mateos, Edificio 9, Col. Lindavista, 07738 México DF, México

H. Villavicencio
Instituto Superior Pedagógico E.J. Varona, La Habana, Cuba
[a] *Permanent Address: Facultad de Física-IMRE, Universidad de la Habana, A. P. 10400, La Habana, Cuba.*

Ternary compounds $Zn_XCd_{1-X}S$ ($0 \le x \le 1$) embedded in a NH4-mordenite zeolite host have been studied by means of photoacoustic techniques to obtain their optical and thermal characterization. Also the chemical composition of these ternary compounds embedded in zeolite host was determinated by EDS. From different Photoacoustic configurations we measure their band-gap energies, thermal diffusivity and thermal effusivity values as a function of the *X* parameter.

.

PACS: 78.20.Hp; 78.20.Wc; 78.40.-q; 78.40.Fy; 78.66.Hf

Keywords: Zeolite mordenite; Photoacoustic spectroscopy; Thermal diffusivity; Thermal effusivity; EDS; Ternary compounds.

1. Introduction

The zeolites are aluminosilicates with a particular framework structure that have enclosed cavities ocuppied with large ions and water molecules which have a considerable freedoom of movement allowing ion exchange and reversible dehydratation [1].

The ternary compounds are frecuently used in the development of optics and optoelectronics devices, in solar cells, high efficiency optical fibers, ligth modulators and diode lasers with blue emission [2]. In the study of compounds embedded in zeolite host (Z-H) we have a wide range of combinations: PbI_2 in faujasite (FAU) [3], T_2O_4Na in Na-A Z-H [4], Methylene Blue CsY Z-H [5], CdS in Zeolite-Y [6], CdS and PbS in Zeolite-Y and Mordenite [7,8] also CdS in $Na_{86}X$ Z-H [9]. The application of the photoacoustic (PA) techniques to porous semiconductors [10], binary and ternary semiconductor compounds have been studied in depth, for example band-gap in thin films [11], band-gap shift in CdS [12] and thermal and structural properties of $Cd_{1-X}Zn_XTe$ [13].

According to Rosencwaig and Gersho (R-G) model [14], the Photoacoustic effect is based in the acoustic signal generated in a gas (air, generally) inside of an air-tight cell. This signal is due to a modulated light absorption by the sample and is detected in the cell by a microphone. When radiation is absorpted, the sample arrive to its excited levels, which to decays, among others, in non-radiative way to cause a local periodic heat flux, modulating the local temperature. So, is generated a mechanical effect of periodical gas expantion-contraction (sound waves) in the PA cell. In all cases, the sound is detected by a microphone coupled to the cell.

In this work we use photoacustic spectroscopy (PAS) to obtain the thermal diffusivity, the thermal effusivity and band-gap of ternary semiconductor $Zn_xCd_{1-x}S$ embedded in NH_4-mordenite (zeolite host) as a function of x (Zn concentration). The samples have been also analyzed by EDS in order to obtain their real composition of the samples (the real x values).

2. Theory and Experiment

2.1 Samples preparation

Zeolite used in this work was NH_4-mordenite (MOR) sintetized in our laboratory. For $Zn_xCd_{1-x}S$ ($x=0$) sample, the preparation was carried out as follows: 1g of MOR powder was added to 30 ml of $CdCl_2$ (0.1M) and 30 ml of $SC(NH_2)_2$ (0.1 M); this mixture is stirred at room temperature. After that, the mixture was then thorougly washed and dried. Finally, ionic exchange was made at 353 K. For the others x composition, $ZnCl_2$ (0.1M) was added in variable volume of the two salts ($ZnCl_2$ and $CdCl_2$) manteining the total volume constant at 30 ml.

2.2 Thermal diffusivity a

In order to perform the PA measurements for thermal diffusivity, circular pieces of the compound powder (about 300 ± 20 μm thickness, 10 mm radius) were prepared by pressing this at 93.6 MPa. The PA experimental setup consists in a 250 W halogen lamp whose polychromatic beam is mechanically modulated and focused onto the sample which is placed in such a way that close a conventional PA cell [14] The microphone signal from the PA cell is connected to a lock-in amplifier used to register both the amplitude and phase signal; these were recorded as a function of the light modulation frequency *f* in a personal computer. We guarantee the optical opacity of our samples by attaching a thin circular Al foil with thermal paste on these samples. By using the Rosencwaig and Gersho theory, the expression for the PA signal, when the sample is thermally thick ($l_s >> \mu_s$, where l_s is the thickness of the sample and $\mu_s = \sqrt{\alpha_s / \pi f}$ is the thermal diffusion length with α_s and f being the thermal diffusivity of the sample and the light modulation frequency respectively), can be written as [14,15]:

$$V_d = \frac{S_0}{1 + jwRC} \frac{\cosh(l_S \sigma_S)}{\operatorname{senh}(l_S \sigma_S)} (1 - (\cosh(\sigma_g l_g) - \operatorname{senh}(\sigma_g l_g)) \quad (e^{jwt}) \qquad (1)$$

where V_d is the signal from the microphone, $\omega = 2\pi f$, l_g is the thickness of the PA chamber, $\sigma_i = (1+j)a_i$ is the complex thermal diffusion coefficient. Here the index i denotes the sample ($i=s$), the air ($i=g$) and the Al foil ($i=0$), in the case of thermal effusivity measurements, with $j = \sqrt{-1}$, $a_i = \sqrt{\pi f / \alpha_i}$ and α_i, k_i, ρ_i, c_i, $_i$ are the thermal diffusivity, thermal conductivity, density, specific heat and thermal effusivity ($e_i = \sqrt{k_i \rho_i c_i}$) of medium i. S_0 is a constant that depends of the PA cell geometry, R and C are the resistance and capacitance of the microphone. The thermal diffusivity values of the samples were obtained by fitting the PA signal amplitude to equation (1) as a function of f.

2.3 Thermal Effusivity e

For thermal effusivity measurements, the samples were the same that those used in the thermal diffusivity measurements. By using the PA configuration and procedure described by Veleva et. al. [16] is possible to obtain the thermal effusivity of these samples. In this case a modulated light beam was focused onto Al disc (thickness $l_0 = 100$ μm) and the sample was attached in the opposite illuminated side with thermal paste. From the Rosencwaig-Gersho theory the PA signal for this configuration can be expressed as [14]:

$$T(x,t) \equiv \theta_g(x) \exp(jwt) = \theta \exp(-\sigma_0 x) \exp(jwt) \qquad (2)$$

with

$$\theta = \frac{\beta I_0}{k_0 \sigma_0} \left\{ \frac{(1+\bar{b}) \exp(l_0 \sigma_0) + (1-\bar{b}) \exp(-l_0 \sigma_0)}{(1+\bar{b}) \exp(l_0 \sigma_0) - (1-\bar{b}) \exp(-l_0 \sigma_0)} \right\} \qquad (3)$$

where β is the optical absorption coefficient, I_0 is the light source also

$$\bar{b} = b \tanh(l_S \sigma_S) \qquad (4)$$

with

$$b = \frac{k_s \sigma_s}{k_0 \sigma_0} = \frac{\sqrt{(k_s \rho_s c_s)}}{\sqrt{(k_0 \rho_0 c_0)}} = \frac{e_s}{e_0}$$

In the frequency range where the sample is thermally thick ($l_s \sigma_s >> 1$) the equation (3) can be written as:

$$\theta = \frac{b I_0}{k_0 l_0 \sigma_0^2} \left(\frac{1}{1 + b/(l_0 \sigma_0)} \right) \qquad (5)$$

For the case in which only the Al disc close the PA cell then the PA signal is reduced to [16]:

$$\theta_0 = \frac{b I_0}{k_0 l_0 \sigma_0^2} \qquad (6)$$

From the ratio between equations (5) and (6), we obtain:

$$\frac{\theta}{\theta_0} = \frac{1}{1 + b/(l_0 \sigma_0)} \qquad (7)$$

Then the thermal effusivity value for each sample was obtained from the fitting the experimental signal ratio to equation (7) as a function of the frequency f.

2.4 Band-gap

The photoacoustic optical absorption spectra were obtained in the 300-700 nm region by using a standard PA spectrometer which consists of a Xe lamp (1000 W), a variable frequency mechanical chopper (set at 17 Hz), a monochromator, a photoacoustic cell with a microphone. The powder sample was placed onto the cilindric chamber and the PA signal obtained was detected by a lock-in amplifier (SR-850), interfaced to a personal computer, which simultaneously displays the wavelength-dependent signal amplitude and phase obtaining then the absorption spectra of the samples (figure 1).

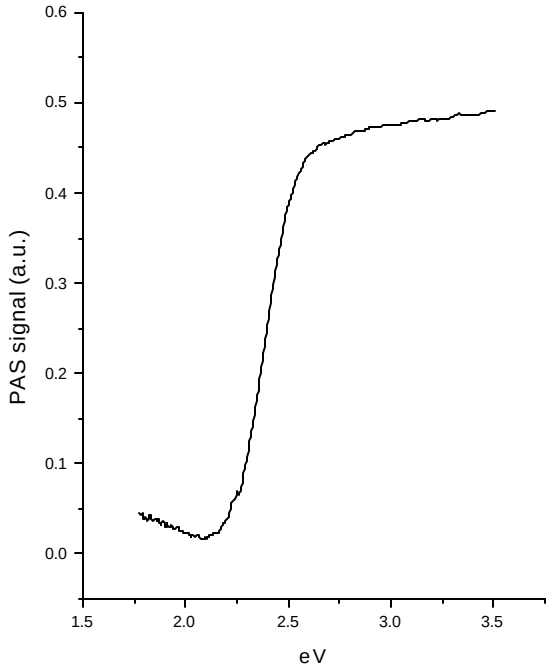

Fig.1 PA spectrum for $Zn_{0.15}Cd_{0.85}S$ embedded in NH_4-mordenite

Each band gap value was obtained by considering that the band gap energy is given at the position where occurs the maximum derivative in the edge of this PA spectrum (fig.2)

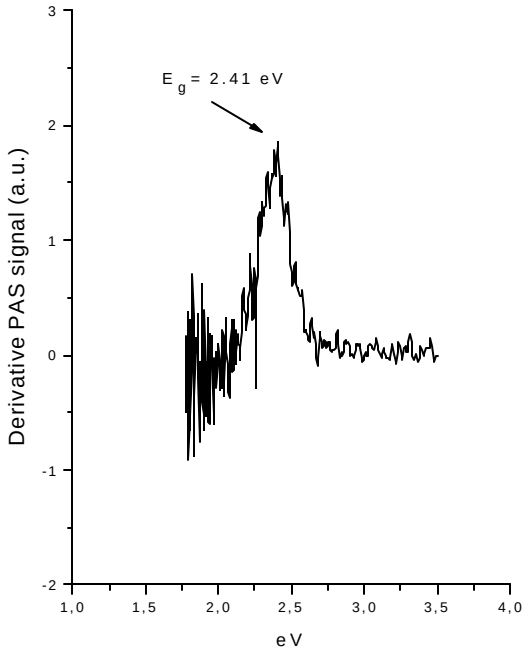

Fig.2 Derivative PAS spectrum for $Zn_{0.15}Cd_{0.85}S$ embedded in NH_4-mordenite

3. Results and discussion

3.1 Thermal diffusivity and effusivity.

We found that there is a relative maximum value for thermal diffusivity and effusivity at low Zn concentration ($0 < x < 0.2$). For x values greather than 0.3, we have that α and ε values are increased, specially for the sample with $x = 0.64$ where we found the maximum value; the results appears in figure 3 and figure 4.

The X-ray diffraction patterns of our samples, not show here, indicate that was maintained the structure of the mordenite host for all the samples (the position of the spectral lines were maintained), however the peak intensities were sensitive to the X value of the ternary compounds embedded in these zeolites as indicative of the influence of the growth of $Zn_XCd_{1-X}S$ compounds, this behavior has been observed in others semiconductor compounds embedded in zeolites [8].

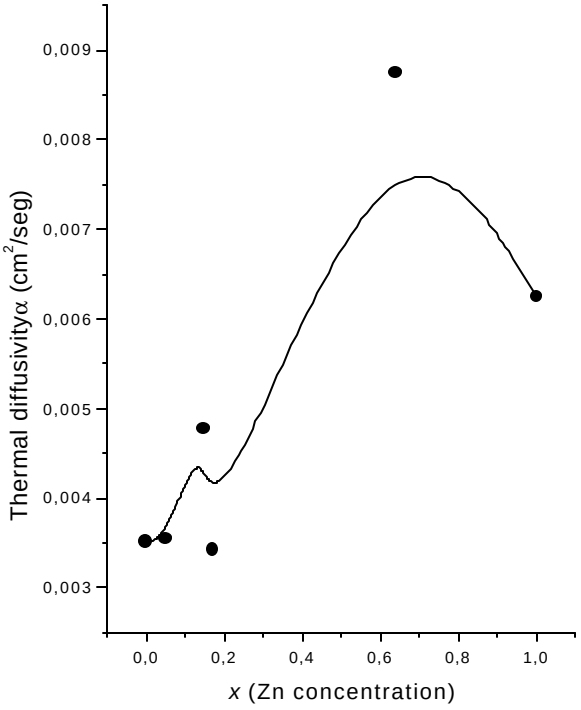

Figure 3. Thermal diffusivity versus Zn concentration. In this case the dots are the obtained thermal diffusivity values and the continuous line indicates the tendency of this thermal property.

It should be stressed that our thermal diffusivity values are similar with those reported in the literature for CdS embedded in Na-Y Z-H [9]. In ref. [17], is reported a maximum for electrical conductivity in x = 0.60, in $Zn_xCd_{1-x}S$ ternary compound this could explain the maximum value in and obtained in our samples. In general we have a parallel behavior between the electrical and thermal properties in a wide range of temperatures

especially at room temperature. In the case of low Zn concentrations it has been reported in the literature [13] that for a similar II-VI ternary compound ($Zn_xCd_{1-x}Te$) have an important increment in its thermal properties at low Zn concentrations, it can be seen as the addition of Zn to CdTe which strengthen the Cd-Te bond [18]. Similar behaviour we can expect in our ternary compound which give a relative maximum in the thermal properties at low Zn concentrations.

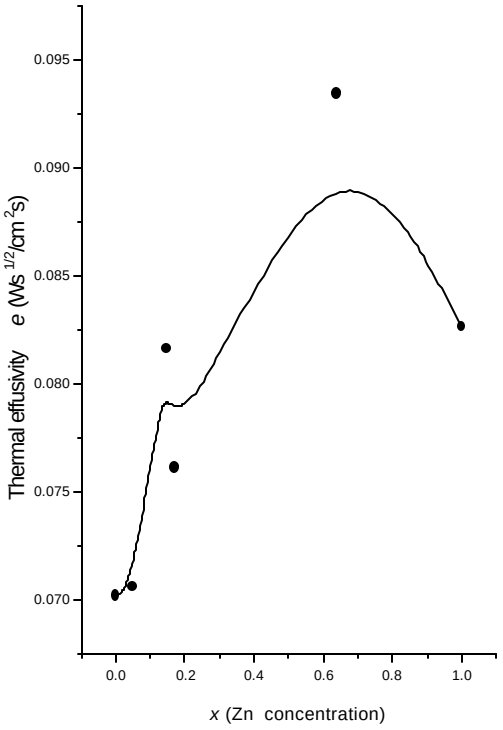

Fig. 4. Thermal effusivity versus Zn concentration. In this case the dots are the obtained thermal effusivity values and the continuous line indicates the tendency of this thermal property.

With these results, we can also calculate the thermal conductivity *k* and heat capacity by unit volume ρc, shown in table 1.

X % Zn	E_g eV	α cm^2/s $x10^{-3}$	ε $Ws^{1/2}/cm^2K$ $x10^{-2}$	*k* W/cmK $x10^{-3}$	ρc Ws/cm^3K
0.00	2.41	3.51	7.01	4.16	1.18
0.05	2.44	3.54	7.05	4.20	1.19
0.15	2.39	4.77	8.16	5.64	1.18
0.17	2.42	3.42	7.61	4.45	1.30
0.64	2.55	8.75	9.34	8.74	1.00
1.00	3.18	6.25	8.26	6.53	1.04

Table 1. Complete results (band gap and thermal parameters)

3.2 Band gap

Figure 5 shows the band gap energy of our samples at room temperature as a function of the *x* parameter. It can be seen in this figure a parabolic behaviour of the band gap energy vs *x* which is characteristic of ternary compounds as $Zn_xCd_{1-x}Se$ [19] and $Al_xGa_{1-x}As$ [20]. The general behavior of the fitting curve, can be described by the parabolic curve:

$$E_g(x) = 2.45561 + 0.7105x - 1.51101x(1-x) \quad (9)$$

which is shown as a continuous line in the figure 5. This behaviour is according with the virtual-crystal approximation which predicts a quadratic dependence respect with *x* [19].

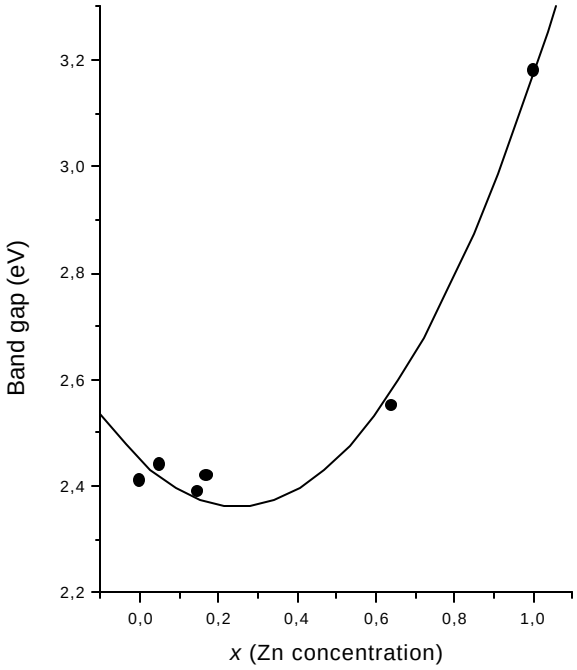

Figure 5. Band gap versus Zn concentration. The dots representes the experimental band gap values and the continuous line the best fitting (Eq. 9).

We observe that the band gap at *x=0* is $E_g(x) = 2.41$ *eV*, this is very close to the measured value (also with PAS) of the CdS band gap $E_g = 2.4$ *eV* [11], but there is a little difference in E_g could be due to the presence of the zeolite host.

Conclusions

Through PAS we found the band gap energy (E_g values) of $Zn_xCd_{1-x}S$ ternary compound embedded in a MOR zeolite host. The band gap was sensitive to the Zn concentration,

even with the compound embedded in a zeolite host.

For the measurement of the thermal diffusivity α and thermal effusivity e we can observ an important variation at low Zn concentration, and its maximum value in $x = 0.6$. From the thermal diffusivity α and the thermal effusivity e of our samples we obtained a completely thermal characterization. Also we obtain the real composition of $Zn_xCd_{1-x}S$ in the zeolite host by using EDS.

Acknowledgements

This work was partially supported by CONACyT-México. The authors are greateful to Eng. Esther Ayala Maycotte, Eng. Marcela Guerrero and EDS staff laboratory of Physics Dept. at CINVESTAV-IPN and the partial finantial support of CICATA-IPN.

References

[1] J. V. Smith in: *Zeolite Chemistry and Catalysis.* Rabo J. A. (editor) ACS Monograph 171, Washington, D.C., 1976.

[2] S. L. Chuang. *Physics of optoelectronics devices.* John Wiley & Sons, New York, 1995.

[3] Z. Kang Tang, Y. Nozu and T. Goto, J. Phys. Soc. Jpn. **60**, 2090, (1991).

[4] K. Tai No, J. Sup Kim, Y. Young Huh, W. Kyeu Kim and M. Shik Jhon, J. Phys. Chem. **60**, 740 (1987).

[5] D. Ho Park, K.W. Lee and S. Joon Choe, Bull. Korean Chem. Soc. **16,** 467 (1995)

[61]W. Chen, Z. Lin, Z. Wang and L. Lin, Solid State Commun. **100,** 101 (1996)

[7] Y. Wang, and N. Herron, J. Phys. Chem. **91,** 257 (1987)

[8] T. Moyo, K. Maruyama and H. Endo, J. Phys. Condens. Matter, **4,** 5653 (1992)

[9] G. Gutiérrez-Juárez, O. Zelaya-Angel, J.J. Alvarado-Gil, H. Vargas, H. de O. Pastore, J. S. Barone, M. Hernández-Velez and L. Baños, J. Chem. Soc. Faraday Trans. **92,** 2651, (1996)

[10] A. Calderón, J.J. Alvarado-Gil, Yu. G. Gurevich, A. Cruz-Orea, I. Delgadillo, H. Vargas, L.C.M. Miranda, Phys. Rev. Lett., **79**, 5022 (1997).

[11] A. Mandelis in: *Photoacoustic and Thermal Wave Phenomena in Semiconductors.* Edit. A. Mandelis (North Holland, New York, 1987.)

[12] O. Zelaya-Angel, J.J. Alvarado-Gil, R. Lozada-Morales, H. Vargas, A. Ferreira da Silva, Appl. Phys. Lett. **64,** 291 (1994)

[13] M.E. Rodríguez, J.J. Alvarado-Gil, I. Delgadillo, O. Zelaya, H. Vargas, F. Sánchez-Sinencio, M. Tufiño-Velázquez and L. Baños, Phys. Stat. Sol. (A) **158,** 67 (1996)

[14] A. Rosencwaig, A. Gersho, J. Appl. Phys. **47,** 64 (1976)

[15] A. Hernández-Guevara, *Application and development of photoacoustic techniques for the determination of thermal and optical properties of semiconductors compound* (In spanish) PhD Thesis CINVESTAV-IPN 2000.

[16] L. Veleva, S.A. Tomás, E. Marín, A. Cruz-Orea, I. Delgadillo, J.J. Alvarado-Gil, P. Quintana, R. Pomés, F. Sánchez, H. Vargas and L.C.M. Miranda, Corrosion Science **39,** 1641 (1997)

[17] J. M. Doña, J. Herrero,Thin Solid Films **268,** 5. (1995)

[18] S.B. Qadri, E. F. Skelton, A. W. Webb, Appl. Phys. Lett., **46,** 257 (1985)

[19] C. Morales-Merino in: *Transition Phase Study and Band Gap variation in* $Zn_XCd_{1-X}Se$ *semiconductor compound.* (In Spanish) M. Sc. Thesis ESFM-IPN 1998.

[20] J.A. Van Vechten, T.K. Bergstresser, Phys. Rev. B, **1,** 3351 (1970)